



*Supplement of*

**Increased importance of aerosol–cloud interactions for surface  $\text{PM}_{2.5}$  pollution relative to aerosol–radiation interactions in China with the anthropogenic emission reductions**

Da Gao et al.

*Correspondence to:* Bin Zhao (bzhao@mail.tsinghua.edu.cn)

The copyright of individual parts of the supplement might differ from the article licence.

## 1 Section 1. The improvement for nitrate simulation

2 Before starting this work. We noted the poor ability of nitrate  
3 simulation in the WRF-Chem model. Previous studies reported that the  
4 nitrate underestimation might be attributed to the HONO underestimation  
5 (Wang et al., 2015; Xue et al., 2020). The source of HONO is originally  
6 from some gas-phase chemical reactions in the WRF-Chem, but other  
7 HONO sources are lacking, such as hydrolysis of NO<sub>2</sub> on humid aerosol  
8 surfaces and heterogeneous conversion of NO<sub>2</sub> on ground surfaces. It also  
9 has been confirmed that these reactions could occur in the atmosphere (Li  
10 et al., 2018, Liu et al., 2019). We added these four heterogeneous HONO  
11 reactions to the WRF-Chem model (Table S1). The addition of these four  
12 reactions enhances atmospheric oxidant and promotes OH radical  
13 formation, thereby promoting the formation of gaseous nitric acid through  
14 strong OH radicals reacting with NO<sub>2</sub>. In addition, the reactions of  
15 hydrolysis of NO<sub>2</sub> on humid aerosol surfaces contributed extra nitric acid.  
16 More nitric acid is beneficial for nitrate formation through condensation  
17 and heterogeneous reactions. Other specific information can be found in  
18 Zhang et al. (2021).

19  
20 Table S1. Heterogeneous HONO reactions added in WRF-Chem (from  
21 Zhang et al., 2021).

number	Reaction	Reference
(1)	$\text{NO}_2 + \text{aerosol} = 0.5 \times \text{HONO} + 0.5 \times \text{HNO}_3$	Liu et al., (2019)

(2)	$\text{NO}_2 + \text{aerosol} = 0.5 \times \text{HONO} + 0.5 \times \text{HNO}_3$	Liu et al., (2019)
(3)	$\text{NO}_2 + \text{ground} = \text{HONO}$	Li et al., (2018), Liu et al., (2019)
(4)	$\text{NO}_2 + \text{ground} + h\nu = \text{HONO}$	Liu et al., (2019)

22

23 Table S2. Regional total emissions of gas and primary particulate matter in  
24 China in 2013 and 2021 and its decrease ratio from 2013 to 2021.

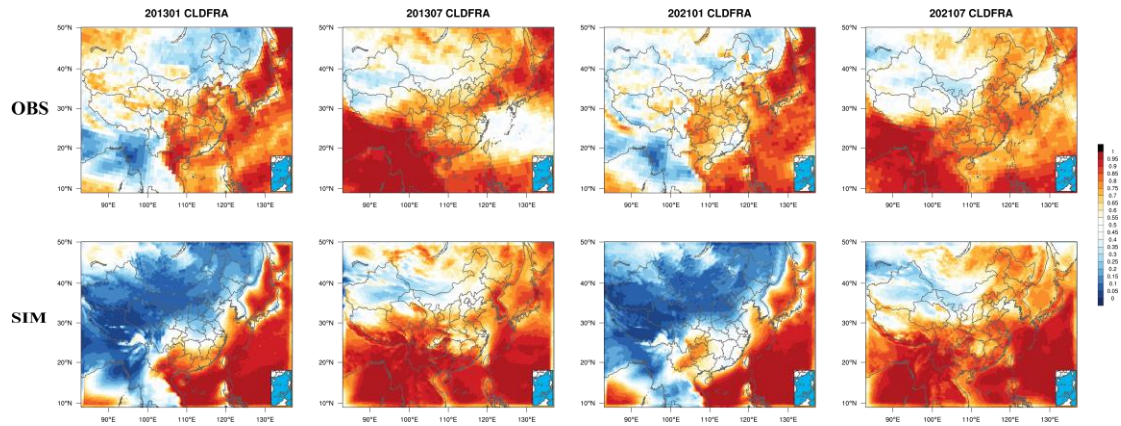
	SO <sub>2</sub>	NO <sub>x</sub>	NH <sub>3</sub>	PM <sub>2.5</sub>	VOCs
2013 (unit: kt)	22402	27753	11040	12536	25330
2021 (unit: kt)	5640	15096	8847	6445	22398
(2013-2021)/2013	75%	46%	20%	49%	12%

25

26 Table S3. Statistics for the simulation of meteorological factors in January  
27 and July of 2013 and 2021.

Meteorological factors		OBS	SIM	Bias
T2 (°C)	January 2013	269.23	269.10	-0.76
	January 2021	270.56	269.97	-0.59
	July 2013	298.02	297.16	-0.86
	July 2021	298.55	297.65	-0.90
Q2 (g/kg)	January 2013	2.47	2.38	-0.09
	January 2021	2.54	2.46	-0.09
	July 2013	14.86	14.71	-0.15
	July 2021	16.30	15.58	-0.72
WS10 (m/s)	January 2013	2.38	3.31	0.94
	January 2021	2.68	3.68	1.00
	July 2013	2.62	3.62	1.00
	July 2021	2.69	3.51	0.82
WD10 (°)	January 2013	275.99	282.83	10.27
	January 2021	259.21	251.70	11.46
	July 2013	192.27	183.08	4.86
	July 2021	180.47	157.43	3.96

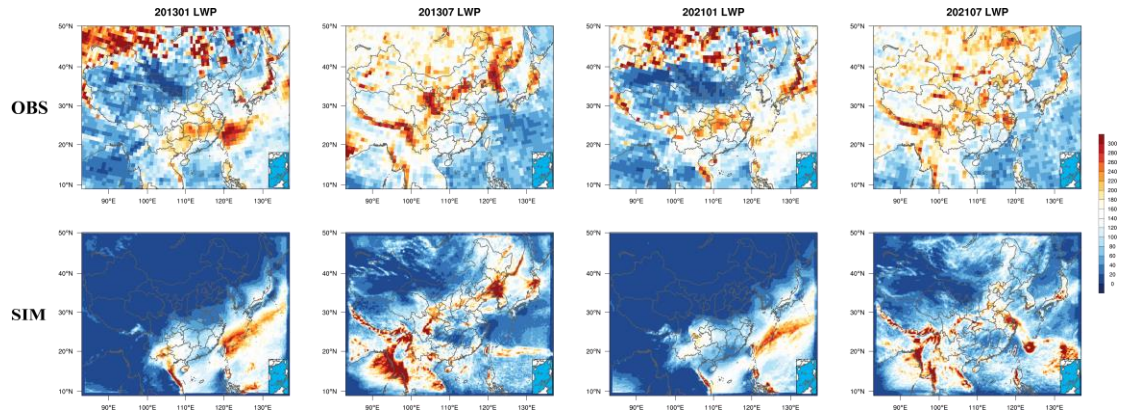
28



29

30 Fig. S1. Observation and simulation of cloud fraction in January and July  
 31 of 2013 and 2021.

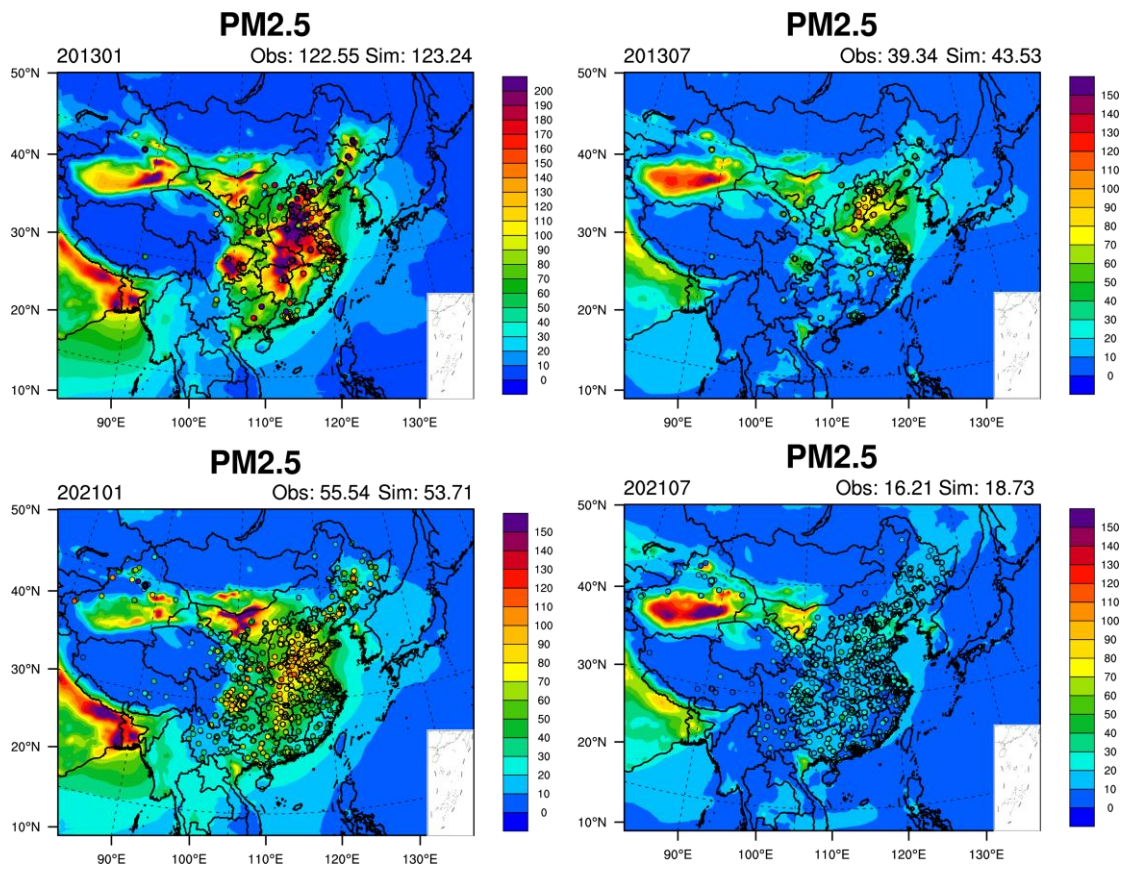
32



33

34 Fig. S2. Observation and simulation of liquid water path (unit:  $\text{g m}^{-2}$ ) in  
 35 January and July of 2013 and 2021.

36

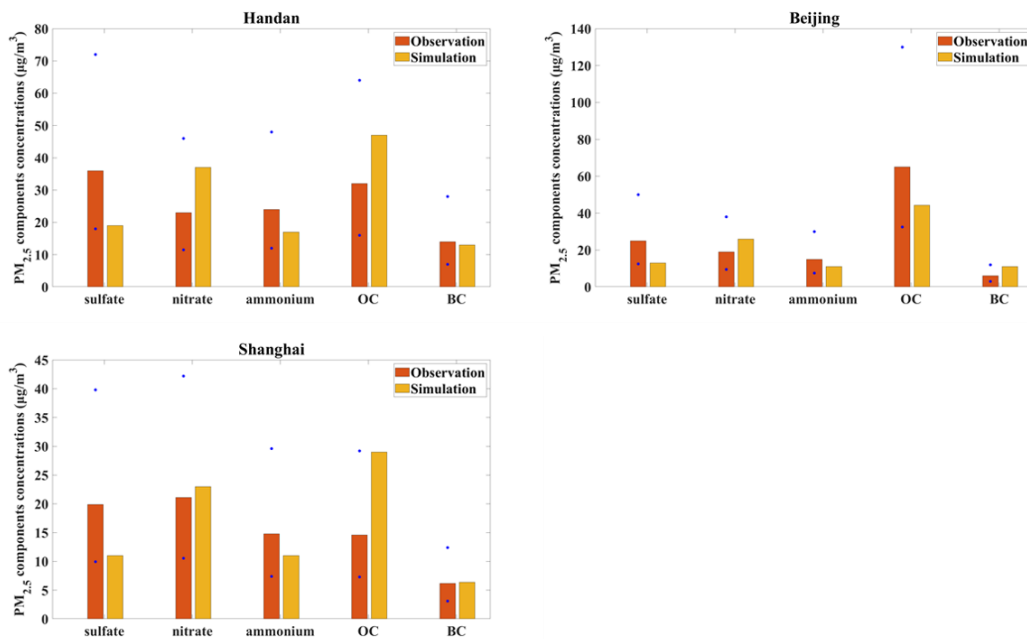


37

38 Fig. S3. Observation and simulation of surface PM<sub>2.5</sub> concentration (unit:

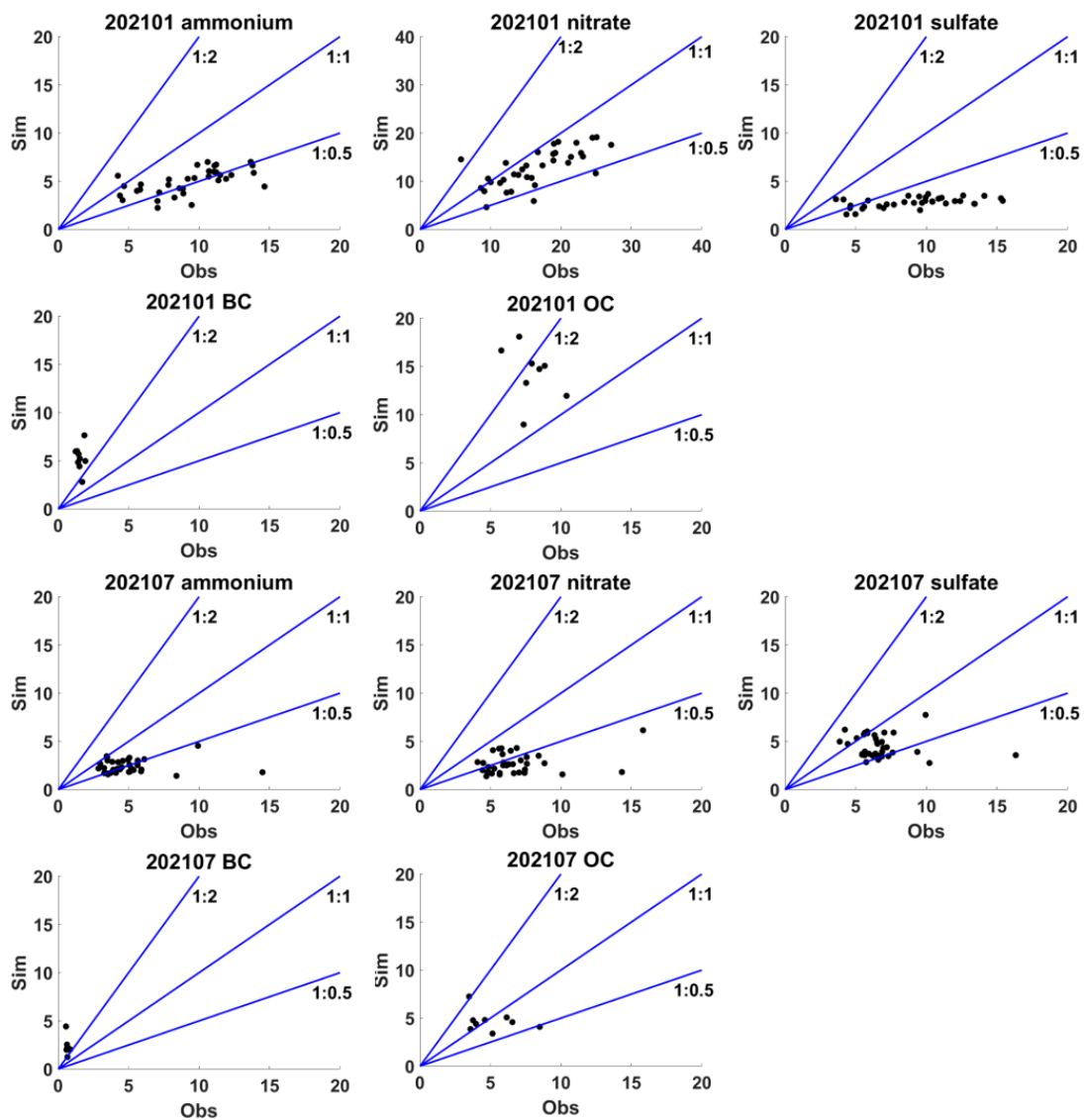
39  $\mu\text{g m}^{-3}$ ) in January and July of 2013 and 2021.

40

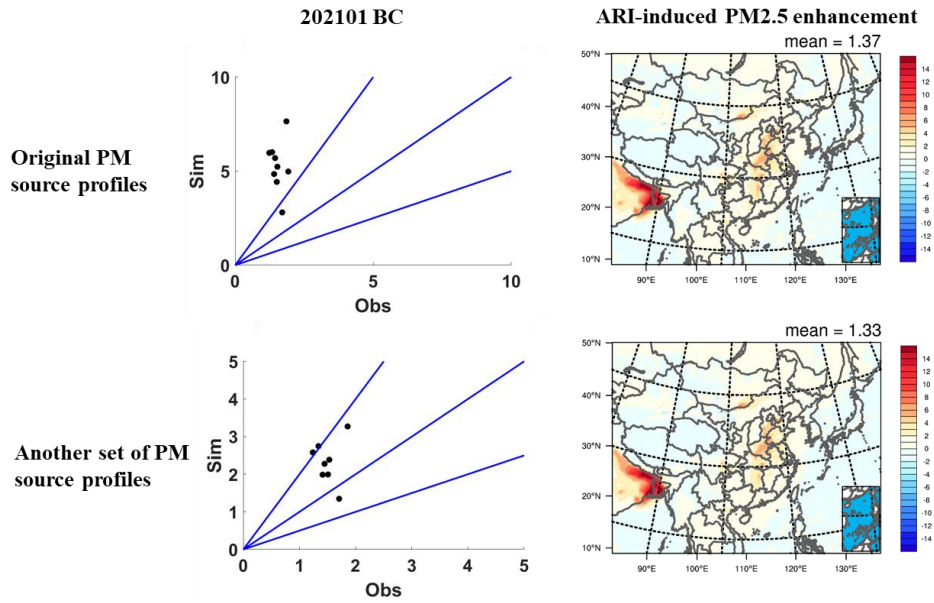


41

42 Fig. S4. Comparisons between PM<sub>2.5</sub> component observations and  
 43 simulations in Handan, Beijing and Shanghai in January 2013. The blue  
 44 points represent double or half of the PM<sub>2.5</sub> component observations. OC  
 45 and BC represent organic aerosol and black carbon.  
 46



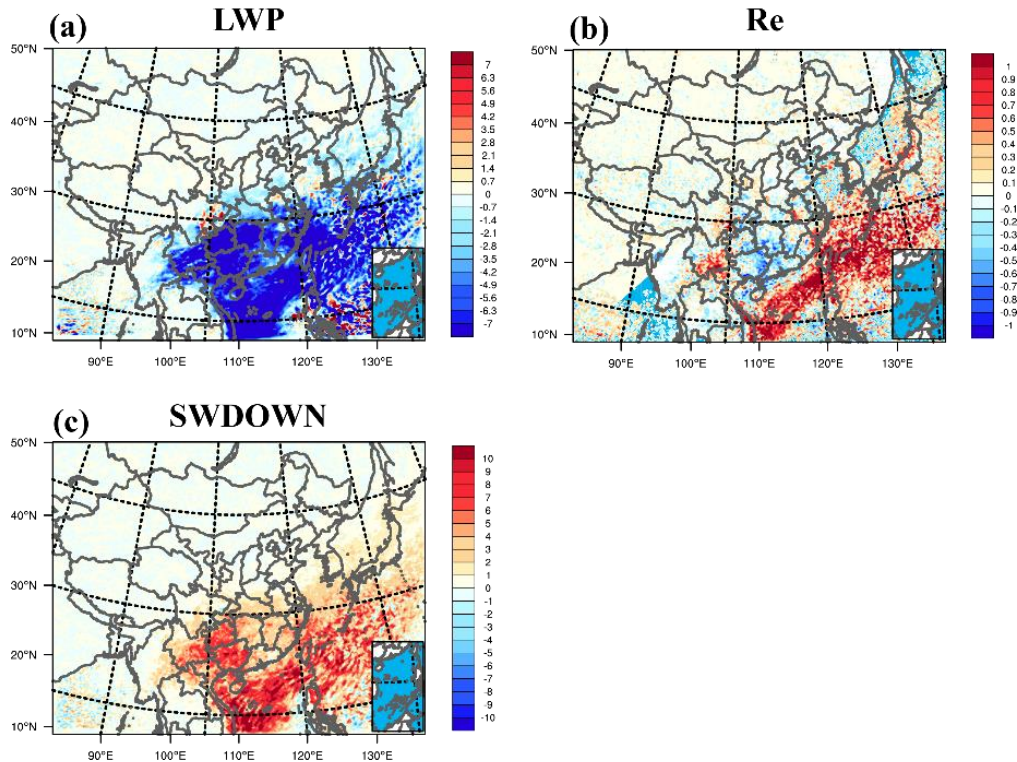
47  
 48 Fig. S5. The ratios of simulation to observation of ammonium, nitrate,  
 49 sulfate, BC and OC (unit:  $\mu\text{g m}^{-3}$ ) in January and July 2021.  
 50



51

52 Fig. S6. The ratios of simulation to observation of BC and ARI-induced  
 53  $PM_{2.5}$  enhancement (unit:  $\mu g m^{-3}$ ) obtained from original PM source  
 54 profiles and another set of PM source profiles in January 2021.

55

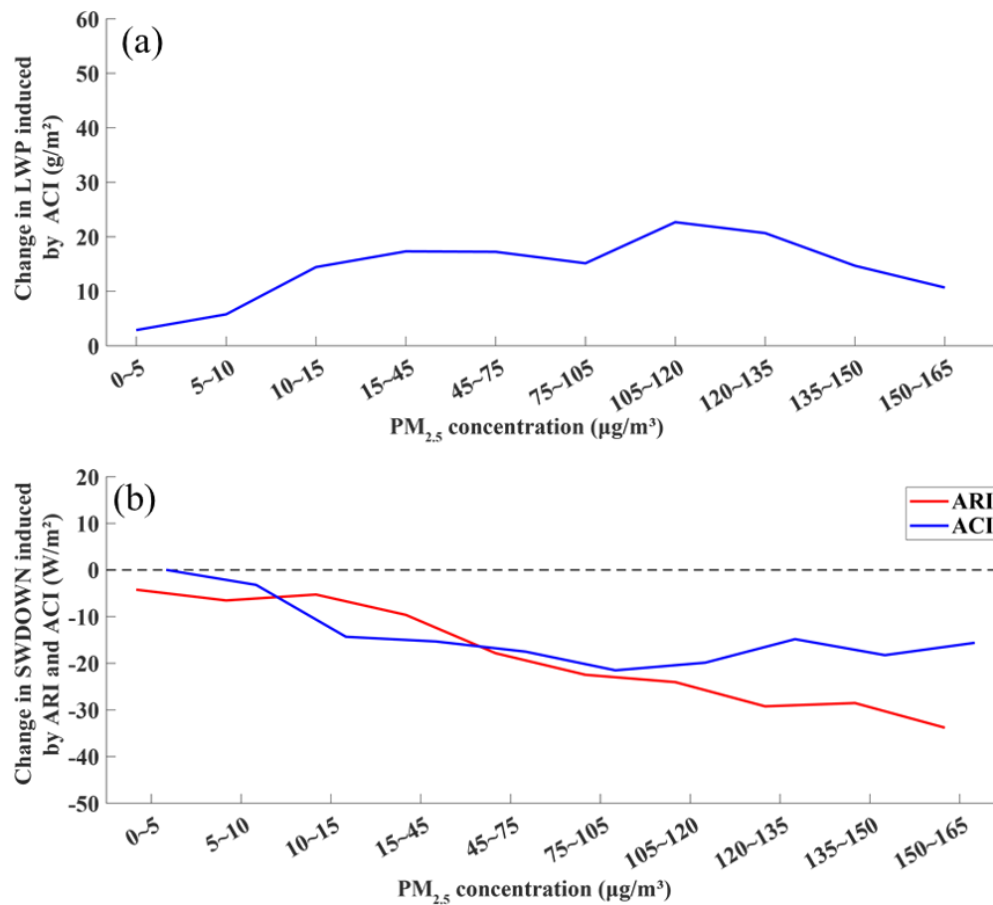


56

57 Fig. S7. Change in aerosol-induced liquid water path (LWP) (unit:  $g m^{-2}$ ),

58 Re (unit:  $\mu\text{m}$ ) and ACI-induced downward shortwave radiation at the  
59 surface (SWDOWN) reduction (unit:  $\text{W m}^{-2}$ ) in January owing to the  
60 emission reduction from 2013 to 2021.

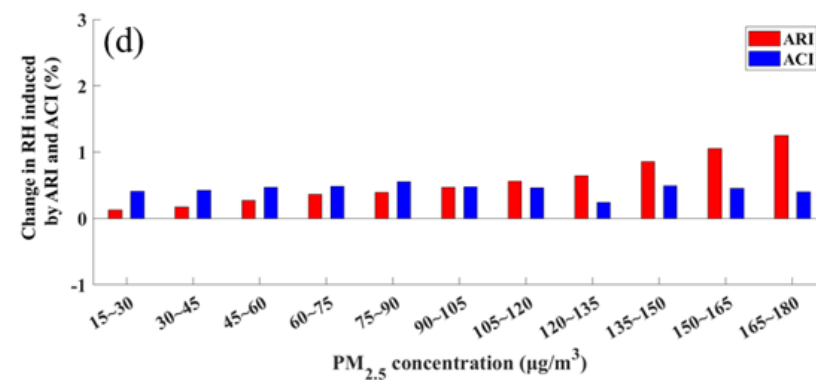
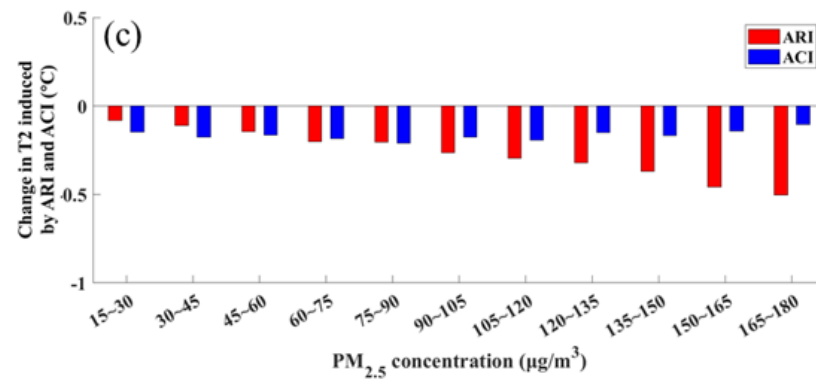
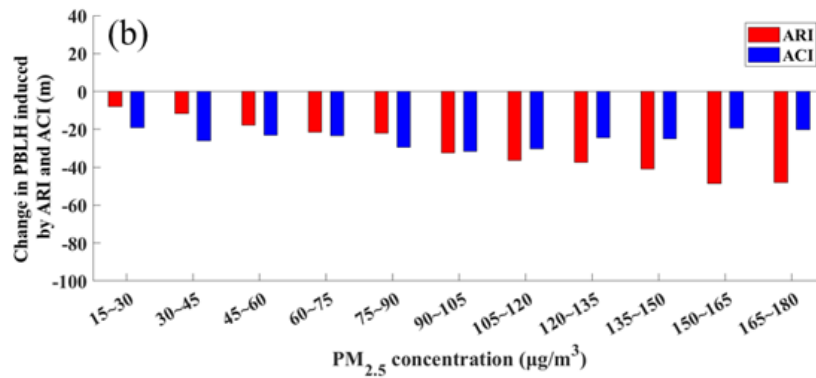
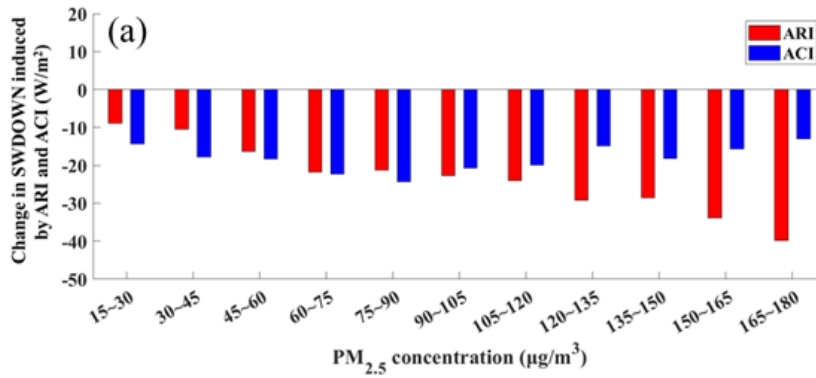
61



62

63 Fig. S8. Change in LWP induced by ACI and SWDOWN induced by ARI  
64 and ACI at different  $\text{PM}_{2.5}$  levels.

65



66

67 Fig. S9. Change in (a) SWDOWN, (b) planetary boundary layer height  
 68 (PBLH), (c) air temperature at 2 m (T2), and (d) relative humidity (RH)

69 induced by ARI and ACI at different ambient PM<sub>2.5</sub> levels. These data are  
70 from the simulations for January and July in the experiments of 21M13E  
71 and 21M21E.

72

### 73 **References**

74 Li, D. D., Xue, L. K., Wen, L., Wang, X. F., Chen, T. S., Mellouki, A., Chen,  
75 J. M., and Wang, W. X.: Characteristics and sources of nitrous acid in  
76 an urban atmosphere of northern China: Results from 1-yr continuous  
77 observations, *Atmos Environ*, 182, 296-306,  
78 10.1016/j.atmosenv.2018.03.033, 2018.

79 Liu, Y. H., Lu, K. D., Li, X., Dong, H. B., Tan, Z. F., Wang, H. C., Zou, Q.,  
80 Wu, Y. S., Zeng, L. M., Hu, M., Min, K. E., Kecorius, S.,  
81 Wiedensohler, A., and Zhang, Y. H.: A Comprehensive Model Test of  
82 the HONO Sources Constrained to Field Measurements at Rural  
83 North China Plain, *Environ Sci Technol*, 53, 3517-3525,  
84 10.1021/acs.est.8b06367, 2019.

85 Wang, L. W., Wen, L., Xu, C. H., Chen, J. M., Wang, X. F., Yang, L. X.,  
86 Wang, W. X., Yang, X., Sui, X., Yao, L., and Zhang, Q. Z.: HONO and  
87 its potential source particulate nitrite at an urban site in North China  
88 during the cold season, *Sci Total Environ*, 538, 93-101,  
89 10.1016/j.scitotenv.2015.08.032, 2015.

90 Xue, C. Y., Zhang, C. L., Ye, C., Liu, P. F., Catoire, V., Krysztofiak, G.,

91       Chen, H., Ren, Y. G., Zhao, X. X., Wang, J. H., Zhang, F., Zhang, C.  
92       X., Zhang, J. W., An, J. L., Wang, T., Chen, J. M., Kleffmann, J.,  
93       Mellouki, A., and Mu, Y. J.: HONO Budget and Its Role in Nitrate  
94       Formation in the Rural North China Plain, *Environ Sci Technol*, 54,  
95       11048-11057, 10.1021/acs.est.0c01832, 2020.

96       Zhang, S. P., Sarwar, G., Xing, J., Chu, B. W., Xue, C. Y., Sarav, A., Ding,  
97       D. A., Zheng, H. T., Mu, Y. J., Duan, F. K., Ma, T., and He, H.:  
98       Improving the representation of HONO chemistry in CMAQ and  
99       examining its impact on haze over China, *Atmos Chem Phys*, 21,  
100       15809-15826, 10.5194/acp-21-15809-2021, 2021.

101